ChemComm

RSC Publishing

COMMUNICATION

View Article Online
View Journal | View Issue

Cite this: *Chem. Commun.*, 2013, **49**, 10730

Received 10th July 2013,
Accepted 26th September 2013

DOI: 10.1039/c3cc45180a

www.rsc.org/chemcomm

A boracite metal–organic framework displaying selective gas sorption and guest-dependent spin-crossover behaviour†

Feng Shao,[a] Jia Li,[a] Jia-Ping Tong,[a] Jian Zhang,[b] Ming-Guang Chen,[a] Zhiping Zheng,*[a] Rong-Bin Huang,[a] Lan-Sun Zheng[a] and Jun Tao*[a]

A metal–organic framework, $[\{Fe(NCS)_2\}_3(TPB)_4]\cdot x$(guest) [$\mathbf{1}\cdot x$(guest), TPB = 1,3,5-tris(4-pyridyl)benzene], shows selective gas adsorption and guest-dependent spin-crossover behaviour.

Metal–organic frameworks (MOFs), featuring metal-containing units linked by appropriate organic linking groups, are a family of porous materials. The pore size can be tuned and various functions may be incorporated into the framework structure. As such, MOF materials have found diverse applications such as in recognition,[1] separation,[2] and storage of guest molecules of interest,[3] sensing,[4] drug delivery,[5] and catalysis.[6] By integrating the porous feature of an MOF with other physical properties, multifunctional materials may be realized with which not only individual propitious traits may be shown collectively, new functions may be generated due to the synergism between different properties.

One physical property of our interest is spin crossover (SCO) or the ability of a material to switch between different electronic spin states upon certain condition changes.[7] Potential applications of this phenomenon include their use in sensory and molecular switch devices. An MOF–SCO marriage would offer the opportunity to explore the bistable electronic configurations and the corresponding magnetic properties that are putatively influenced or even dictated by the guest species occluded in the porous framework. To date, there exist only a few examples in the literature, $[Fe(NCS)_2(L)_2]\cdot n$(guest)[8] and $\{Fe(L)[M(CN)_4]\}\cdot m$(guest) (L = *exo*-dentate dipyridyl ligands; M = divalent Ni, Pd, and Pt)[9] and SCO Prussian Blue analogues (PBs).[10]

We report here the design and synthesis, crystallographic analysis, and magnetic studies of a new SCO–MOF complex composed of $Fe(NCS)_2$ units bridged by the tritopic pyridyl-based ligand 1,3,5-tris(4-pyridyl)benzene (TPB) with the formula $[\{Fe(NCS)_2\}_3(TPB)_4]\cdot x$(guest) [$\mathbf{1}\cdot x$(guest)]. The assembly strategy is illustrated in Fig. 1a. The metal–ligand coordination favours the formation of a porous structure, while the Fe(II) complex unit is responsible for the SCO behaviour. Selective gas sorption and guest-dependent SCO properties have been demonstrated.

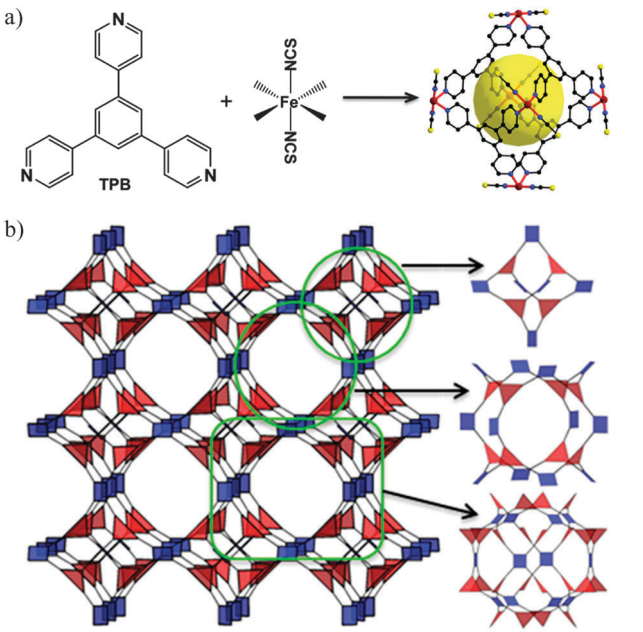

Fig. 1 The assembly of framework **1** showing one unit of the M_6L_4 building blocks (a) and the porous structure of **1** showing three different types of cages (octahedral M_6L_4 and cuboctahedral $M_{12}L_8$ and $M_{12}L_{24}$), where ligand TPB is shown as triangle and the $[FeN_4(NCS)_2]$ moiety shown as square (b).

Complex $\mathbf{1}\cdot x$(guest) crystallizes in the cubic space group $Fm\bar{3}m$. Framework **1** may be viewed as a construct of the octahedral cage-like secondary building units of M_6L_4 (Fig. 1a, right) composed of six Fe vertices and four TPB panels. The Fe atom is located at a site with mmm symmetry, each Fe(II) ion is hexacoordinated with four pyridyl groups of different TPB ligands within the equatorial plane and two axial NCS^- ligands. The adjacent and antipodal Fe–Fe distances in

[a] *State Key Laboratory of Physical Chemistry of Solid Surfaces and Department of Chemistry, College of Chemistry and Chemical Engineering, Xiamen University, Xiamen 361005, People's Republic of China. E-mail: taojun@xmu.edu.cn; Fax: +86-592-2183047; Tel: +86-592-2188138*

[b] *Fujian Institute of Research on the Structure of Matter, Chinese Academy of Science, Fuzhou 350002, People's Republic of China*

† Electronic supplementary information (ESI) available: Information on materials and measurements, synthesis and characterization data, supplementary figures, TG and IR. CCDC 908621 and 908622. For ESI and crystallographic data in CIF or other electronic format see DOI: 10.1039/c3cc45180a

the M_6L_4 cage are 13.24 and 18.72 Å (120 K), respectively. Each Fe vertex is shared by two octahedra. As such, each octahedron is connected to six identical neighbours, resulting in a regular 3D framework with intersecting nanopores (Fig. 1b and Fig. S1–S2, ESI†). Solvent molecules in the as-synthesized crystalline samples are severely disordered and cannot be refined well in our crystallographic analysis. Elemental analysis suggests that $10H_2O$, $15CH_2Cl_2$, and 60EtOH molecules reside in the framework, consistent with the thermogravimetric analysis (Fig. S3, ESI†). Topologically, the present structure closely resembles those of $[Cu_3(TPT)_4](ClO_4)_3$ [TPT = 2,4,6-tris(4-pyridyl)-1,3,5-triazine],[11] $[\{Co(NCS)_2\}_3(TPT)_4]$,[12] and $[Cu_3(BTC)_2(H_2O)_3]$ (BTC = benzene-1,3,5-tricarboxylate),[13] all belonging to the augmented twisted boracite structure.[14] Three types of cages can be identified in the framework structure as shown in Fig. 1b, one smaller octahedral M_6L_4 cage (diameter about 10 Å) and two significantly larger cuboctahedral $M_{12}L_8$ (diameter about 20 Å) and $M_{12}L_{24}$ (diameter about 26 Å) cages formed between the smaller cages. The large openings allow for ready access, passage, and exchange of guest species as subsequently observed.

To assess the porous characteristics of the framework, its performance in N_2 adsorption was recorded following the activation of the as-synthesized sample by supercritical CO_2. Powder X-ray diffraction studies (Fig. S4, ESI†) suggest that the activated sample maintained its crystallinity while the Scanning Electron micrographs (Fig. 2b) clearly reveal its porous features. Its Langmuir and Brunauer–Emmett–Teller (BET) surface areas were found to be 856.66 and 713.68 $m^2\ g^{-1}$, respectively. Its pore volume was determined to be 1.22 $cm^3\ g^{-1}$, with the width maximum being 20 nm. The sorption isotherms at 77 K (Fig. 2a), showing a typical type-IV sorption behaviour,[15] are consistent with the morphological and structural characteristics of the activated sample. The nearly reversible sorption–desorption behaviour may be attributed to the well-structured cylinder-like channels, while the slight hysteresis may be due to the agglomeration of the sample. The rapid increase of N_2 adsorption in the high-pressure region (close to $P/P_0 = 1$) may arise from the substantial inter-particle sorption and the capillary condensation effect.

The capacity of **1** for the uptake of CO_2, CH_4, N_2, and H_2 was measured at 273 K (Fig. 3 and Fig. S5, ESI†). The values are 46.73 $cm^3\ g^{-1}$ for CO_2, 8.32 $cm^3\ g^{-1}$ for CH_4, and 1.80 $cm^3\ g^{-1}$ for N_2, indicating a moderate CO_2–CH_4 selectivity (13.1) and a higher CO_2–N_2 selectivity of 61.2. Adsorption of H_2 was not observed, suggesting that the interaction of H_2 molecules with the host framework is minimal.

The magnetic susceptibilities of the as-synthesized sample measured in an applied field of 5000 Oe are shown in the form of plots of $\chi_M T$ *versus* T (Fig. 4). The measurements were performed using a sample immersed in a mixture of CH_2Cl_2–EtOH (v/v 4 : 1). The sample was cooled from 300 K to 5 K and then warmed up from 5 K to 300 K at a constant rate of 1 K min^{-1} while the susceptibilities were measured at different temperatures. Within the temperature range of 220–100 K, the $\chi_M T$ value changes drastically with hysteresis, suggesting the occurrence of SCO. At 300 K, the $\chi_M T$ value is 3.6 $cm^3\ mol^{-1}$ K, indicating HS Fe(II). Upon cooling, the $\chi_M T$ value first decreases gradually and then with a sudden drop at about 150 K to 1.0 $cm^3\ mol^{-1}$ K at 100 K, following

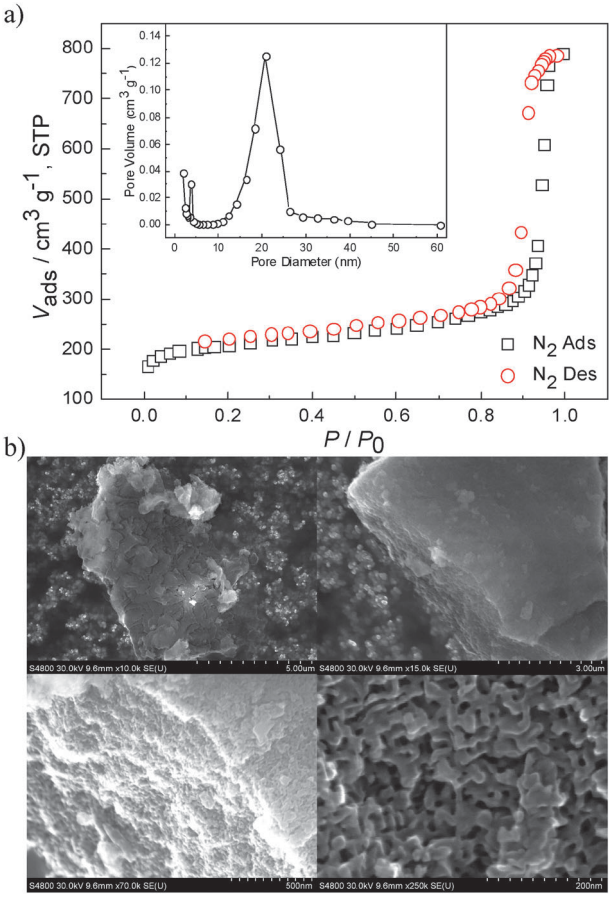

Fig. 2 Adsorption–desorption isotherms of N_2 (77 K) and distribution of pores of activated **1** (a) and SEM images of activated **1** (b).

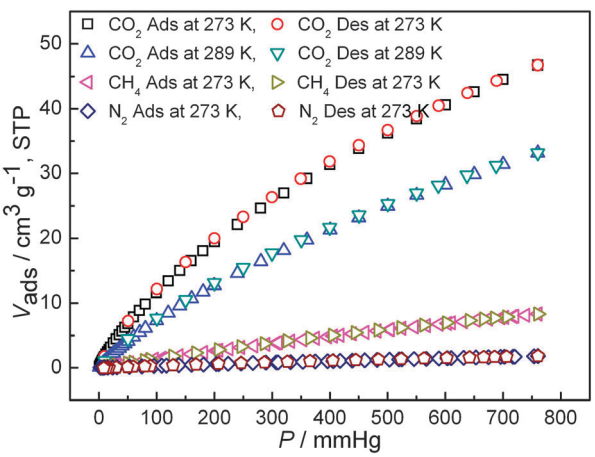

Fig. 3 Adsorption–desorption isotherms of CO_2, CH_4 and N_2 in **1**.

which a more gradual decrease resumes to reach a value of 0.7 $cm^3\ mol^{-1}$ K at 50 K. These results are consistent with a nearly complete SCO process with residual HS Fe(II). The transition temperatures are $T_{c\downarrow}$ = 142 K (cooling mode) and $T_{c\uparrow}$ = 152 K (warming mode), respectively, yielding a hysteresis loop of 10 K.

The SCO transition is accompanied by distinct structural changes. Over the temperature range of 100–220 K within which the SCO behaviour was observed by magnetic studies,

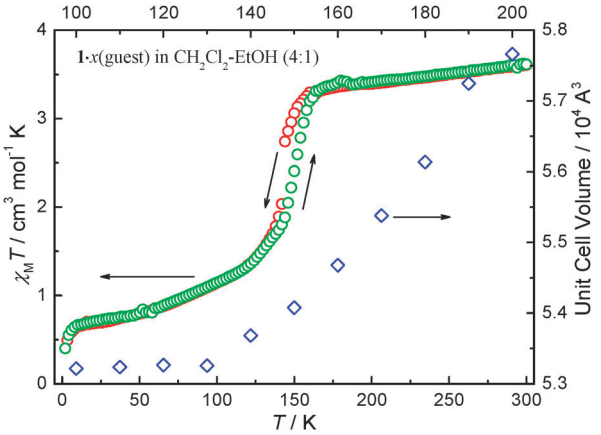

Fig. 4 Plots of $\chi_M T$ *versus* T per Fe(II) ion for **1** in CH_2Cl_2–EtOH (4 : 1) solution and temperature-dependent unit-cell volume of **1**·*x*(guest).

crystallographic analysis revealed, upon temperature increase, a significant increase of 8.4% of the unit-cell volume of **1**·*x*(guest) (Fig. 4). Corresponding to this volume increase is the elongation of the Fe–N bonds. Specifically, the Fe–N_{NCS} and Fe–N_{py} bond lengths are, respectively, 1.938(8) Å and 1.998(5) Å at 120 K, consistent with the presence of LS Fe(II). Upon temperature increase to 173 K, the corresponding metric values showed sizable changes to 2.089(6) Å and 2.221(4) Å, respectively, clearly indicating that the increase of the Fe–N distances is associated with the SCO transition. Over this course the framework structure remains unchanged as no phase transition was observed.

The SCO behaviour of the framework complex appeared to be profoundly dependent on the nature of the guest(s). Upon partial desolvation by supercritical CO_2 (**1**·H_2O, Fig. S6, ESI†) and in a solvent mixture of EtOH–CH_2Cl_2 with a volume ratio larger than 4 : 1 (Fig. S7, ESI†), the SCO behaviour vanished. These observations indicate that the electronic structure of the Fe(II) center is significantly perturbed when interacting with different solvents. In other words, the present framework may serve as a platform to investigate the interplay between guest occlusion and SCO properties.

In summary, we reported herein a novel SCO framework complex. Partial desolvation by supercritical CO_2 afforded the activated material that displayed not only high selectivity of gas sorption toward CO_2 *versus* CH_4 and N_2, but also guest-dependent SCO behaviours. These results suggest the possibility of modifying the SCO properties of this and other metal–organic framework solids by subtly perturbing the guest–framework interactions. More significantly, the present findings portend the realization of multifunctional materials whose applications may include guest-triggered molecular switches, sensors, and guest-specific information storage.

We appreciate the financial support from the NNSF of China (Grants 21021061 and 20923004) and the Specialized Research Fund for the Doctoral Program of Higher Education (Grant 20110121110012).

Notes and references

1 (*a*) B.-L. Chen, S.-C. Xiang and G.-D. Qian, *Acc. Chem. Rev.*, 2010, **43**, 1115; (*b*) H. C. Hoffmann, S. Paasch, P. Müller, I. Senkovska, M. Padmanaban, F. Glorius, S. Kaskel and E. Brunner, *Chem. Commun.*, 2012, **48**, 10484; (*c*) Y. Ikezoe, G. Washino, T. Uemura, S. Kitagawa and H. Matsui, *Nat. Mater.*, 2012, **11**, 1081.
2 (*a*) M. Dinca and J. R. Long, *J. Am. Chem. Soc.*, 2005, **127**, 9376; (*b*) D. Noguchi, H. Tanaka, A. Kondo, H. Kajiro, H. Noguchi, T. Ohba, H. Kanoh and K. Kaneko, *J. Am. Chem. Soc.*, 2008, **130**, 6367.
3 (*a*) H. Li, M. Eddaoudi, M. O'Keeffe and O. M. Yaghi, *Nature*, 1999, **402**, 276; (*b*) M. Kondo, T. Okubo, A. Asami, S. Noro, T. Yoshitomi, S. Kitagawa, T. Ishii, H. Matsuzaka and K. Seki, *Angew. Chem., Int. Ed.*, 1999, **38**, 140; (*c*) K. S. Min and M. P. Suh, *J. Am. Chem. Soc.*, 2000, **122**, 6834; (*d*) A. M. Seayad and D. M. Antonelli, *Adv. Mater.*, 2004, **16**, 765.
4 (*a*) G. J. Haldler, C. J. Kepert, B. Moubaraki, K. S. Murray and J. D. Cashion, *Science*, 2002, **298**, 1762; (*b*) L. E. Kreno, J. T. Hupp and R. P. Van Duyne, *Anal. Chem.*, 2010, **82**, 8042; (*c*) Z.-Z. Lu, R. Zhang, Y.-Z. Li, Z.-J. Guo and H.-G. Zheng, *J. Am. Chem. Soc.*, 2011, **133**, 4172; (*d*) H.-L. Tan, B.-X. Liu and Y. Chen, *ACS Nano*, 2012, **6**, 10505; (*e*) X. Zhu, H.-Y. Zheng, X.-F. Wei, Z.-Y. Lin, L.-H. Guo, B. Qiu and G.-H. Chen, *Chem. Commun.*, 2013, **49**, 1276.
5 (*a*) A. C. McKinlay, R. E. Morris, P. Horcajada, G. Férey, R. Gref, P. Couvreur and C. Serre, *Angew. Chem., Int. Ed.*, 2010, **49**, 6260; (*b*) P. Horcajada, R. Gref, T. Baati, P. K. Allan, G. Maurin, P. Couvreur, G. Férey, R. E. Morris and C. Serre, *Chem. Rev.*, 2012, **112**, 1232.
6 (*a*) J. S. Seo, D. Wand, H. Lee, S. I. Jun, J. Oh, Y. Jeon and K. Kim, *Nature*, 2000, **404**, 982; (*b*) H. R. Moon, J. H. Kim and M. P. Suh, *Angew. Chem., Int. Ed.*, 2005, **44**, 1261; (*c*) C.-D. Wu, A. Hu, L. Zhang and W. Lin, *J. Am. Chem. Soc.*, 2005, **127**, 8940; (*d*) L. Ma, C. Abney and W. Lin, *Chem. Soc. Rev.*, 2009, **38**, 1248.
7 (*a*) B. Li, R.-J. Wei, J. Tao, R.-B. Huang and L.-S. Zheng, *J. Am. Chem. Soc.*, 2010, **132**, 1558; (*b*) B. Li, L.-Q. Chen, R.-J. Wei, J. Tao, R.-B. Huang and L.-S. Zheng, *Inorg. Chem.*, 2011, **50**, 424; (*c*) R.-J. Wei, J. Tao, R.-B. Huang and L.-S. Zheng, *Inorg. Chem.*, 2011, **50**, 8553; (*d*) R.-J. Wei, Q. Huo, J. Tao, R.-B. Huang and L.-S. Zheng, *Angew. Chem., Int. Ed.*, 2011, **50**, 8940.
8 (*a*) S. M. Neville, B. Moubaraki, K. S. Murray and C. J. Kepert, *Angew. Chem., Int. Ed.*, 2007, **46**, 2059; (*b*) S. M. Neville, G. J. Halder, K. W. Chapman, M. B. Duriska, P. D. Southon, J. D. Cashion, J.-F. Létard, B. Moubaraki, K. S. Murray and C. J. Kepert, *J. Am. Chem. Soc.*, 2008, **130**, 2869; (*c*) G. J. Halder, K. W. Chapman, S. M. Neville, B. Moubaraki, K. S. Murray, J.-F. Létard and C. J. Kepert, *J. Am. Chem. Soc.*, 2008, **130**, 17552; (*d*) S. M. Neville, G. J. Halder, K. W. Chapman, M. B. Duriska, B. Moubaraki, K. S. Murray and C. J. Kepert, *J. Am. Chem. Soc.*, 2009, **131**, 12106.
9 (*a*) M. Ohba, K. Yoneda, G. Agustí, M. C. Muñoz, A. B. Gaspar, J. A. Real, M. Yamasaki, H. Ando, Y. Nakao, S. Sakaki and S. Kitagawa, *Angew. Chem., Int. Ed.*, 2009, **48**, 4767; (*b*) R. Ohtani, K. Yoneda, S. Furukawa, N. Horike, S. Kitagawa, A. B. Gaspar, M. C. Muñoz, J. A. Real and M. Ohba, *J. Am. Chem. Soc.*, 2011, **133**, 8600; (*c*) C. Bartual-Murgui, L. Salmon, A. Akou, N. A. Ortega-Villar, H. J. Shepherd, M. C. Muñoz, G. Molnár, J. A. Real and A. Bousseksou, *Chem.–Eur. J.*, 2012, **18**, 507; (*d*) F. J. Muñoz-Lara, A. B. Gaspar, M. C. Muñoz, M. Arai, S. Kitagawa, M. Ohba and J. A. Real, *Chem.–Eur. J.*, 2012, **18**, 8013.
10 (*a*) W. Kosaka, K. Nomura, K. Hashimoto and S.-I. Ohkoshi, *J. Am. Chem. Soc.*, 2005, **127**, 8590; (*b*) D. Papanikolaou, S. Margadonna, W. Kosaka, S.-I. Ohkoshi, M. Brunelli and K. Prassides, *J. Am. Chem. Soc.*, 2006, **128**, 8358; (*c*) C. Avendano, M. G. Hilfiger, A. Prosvirin, C. Sanders, D. Stepien and K. R. Dunbar, *J. Am. Chem. Soc.*, 2010, **132**, 13123; (*d*) S.-I. Ohkoshi and H. Tokoro, *Acc. Chem. Res.*, 2012, **45**, 1749.
11 B. F. Abrahams, S. R. Batten, H. Hamit, B. F. Hoskins and R. Robson, *Angew. Chem., Int. Ed. Engl.*, 1996, **35**, 1690.
12 Y. Inokuma, T. Arai and M. Fujita, *Nat. Chem.*, 2010, **2**, 780.
13 S. S.-Y. Cui, S. M.-F. Lo, J. P. H. Charmant, A. G. Orpen and I. D. Williams, *Science*, 1999, **283**, 1148.
14 (*a*) S. R. Batten, S. M. Neville and D. R. Turner, *Coordination Polymers: Design, Analysis and Application*, RSC Publishing, Cambridge, UK, 2009, pp. 48; (*b*) O. Delgado-Friedrichs, M. O'Keeffe and O. M. Yaghi, *Acta Crystallogr.*, 2006, **A62**, 350; (*c*) H. Furukawa, Y. B. Go, N. Ko, Y. K. Park, F. J. Uribe-Romo, J. Kim, M. O'Keeffe and O. M. Yaghi, *Inorg. Chem.*, 2011, **50**, 9147.
15 K. S. W. Sing, D. H. Everett, R. A. W. Haul, L. Mouscou, J. Rouquerol and I. Siemieniewska, *Pure Appl. Chem.*, 1985, **57**, 603.

